Tranilast Inhibits Hormone Refractory Prostate Cancer Cell Proliferation and Suppresses Transforming Growth Factor β1-Associated Osteoblastic Changes

Kouji Izumi,[1] Atsushi Mizokami,[1]* You Qiang Li,[1] Kazutaka Narimoto,[1] Kazuhiro Sugimoto,[1] Yoshifumi Kadono,[1] Yasuhide Kitagawa,[1] Hiroyuki Konaka,[1] Eitetsu Koh,[1] Evan T. Keller,[2] and Mikio Namiki[1]

[1]*Department of Integrative Cancer Therapy and Urology, Kanazawa University Graduate School of Medical Science, Kanazawa, Japan*

[2]*Department of Urology, School of Medicine, University of Michigan Health System, Ann Arbor, Michigan*

BACKGROUND. Tranilast is a therapeutic agent used in treatment of allergic diseases, although it has been reported to show anti-tumor effects on some cancer cells. To elucidate the effects of tranilast on prostate cancer, we investigated the mechanisms of its anti-tumor effect on prostate cancer.

METHODS. The anti-tumor effects and related mechanisms of tranilast were investigated both in vitro on prostate cancer cell lines and bone-derived stromal cells, and in vivo on severe combined immunodeficient (SCID) mice. We verified its clinical effect in patients with advanced hormone refractory prostate cancer (HRPC).

RESULTS. Tranilast inhibited the proliferation of LNCaP, LNCaP-SF, and PC-3 cells in a dose-dependent manner and growth of the tumor formed by inoculation of LNCaP-SF in the dorsal subcutis and in the tibia of castrated SCID mice. Flow cytometry and TUNEL assay revealed induction of cell cycle arrest and apoptosis by tranilast. Tranilast increased expression of proteins involved in induction of cell cycle arrest and apoptosis. Coculture with bone-derived stromal cells induced proliferation of LNCaP-SF cells. Tranilast also suppressed secretion of transforming growth factor β1 (TGF-β1) from bone-derived stromal cells, which induced their differentiation. Moreover, tranilast inhibited TGF-β1-mediated differentiation of bone-derived stromal cells and LNCaP-SF cell migration induced by osteopontin. In the clinical investigation, PSA progression was inhibited in 4 of 16 patients with advanced HRPC.

CONCLUSIONS. These observations suggest that tranilast may be a useful therapeutic agent for treatment of HRPC via the direct inhibitory effect on cancer cells and suppression of TGF-β1-associated osteoblastic changes in bone metastasis. *Prostate 69: 1222–1234, 2009.*

KEY WORDS: **prostate cancer; tranilast; and TGF-β**

INTRODUCTION

Prostate cancer is the most frequently diagnosed cancer and the second leading cause of cancer-related death in the USA [1]. Skeletal metastases occur in approximately 80% of patients with advanced prostate cancer, and no curative therapies are available for advanced prostate cancer [2,3]. Although hormone therapy is useful, its effects are limited because prostate cancer changes to an androgen-independent phenotype over several years of therapy [4,5]. It is extremely

Grant sponsor: Ministry of Education, Culture, Sport, Science, and Technology of Japan; Grant sponsor: National Institutes of Health; Grant number: P01 CA093900.

*Correspondence to: Atsushi Mizokami, Department of Integrative Cancer Therapy and Urology, Kanazawa University Graduate School of Medical Science, 13-1 Takara-machi, Kanazawa, Ishikawa 920-8641, Japan. E-mail: mizokami@med.kanazawa-u.ac.jp

Received 12 February 2009; Accepted 6 April 2009
DOI 10.1002/pros.20975
Published online 11 May 2009 in Wiley InterScience (www.interscience.wiley.com).

difficult to cure hormone refractory prostate cancer (HRPC) with no clear consensus about the appropriate management strategy. Recently, some oral salvage therapies, such as alternative anti-androgens, estramustine phosphate (EMP), and dexamethasone (DEX) for HRPC have been reported [6–8]. However, as their effects do not last for a long time, new agents are required for the treatment of advanced HRPC.

Bone is constantly being remodeled and releases potential chemoattractants for tumor cells [9]. The growth rate of prostate cancer cells accelerates once they enter the bone environment, suggesting that factors are present in bone that stimulate tumor proliferation [10]. In the bone marrow, several growth factors and cytokines are produced by osteoblasts and are incorporated into the bone matrix [11]. Transforming growth factor β (TGF-β) is known to play an extremely important role in the local modulation of bone metabolism [12]. TGF-β1 is released by osteoblasts and bone stromal cells and is a potent paracrine stimulator of prostate cancer growth in bone metastasis. Bone-derived TGF-β1 forms a vicious cycle to promote the development and progression of bone metastasis. In early tumorigenesis, TGF-β is a tumor suppressor, but advanced cancers lose their growth inhibition and are often stimulated to metastasize by TGF-β [13]. Yonou et al. [14] demonstrated that the serine protease activity of prostate-specific antigen (PSA) stimulated osteoblast proliferation, differentiation, and secretion of TGF-β from osteoblasts, and simultaneously decreased the number of osteoclasts.

We encountered a case in which progression of serum PSA of the HRPC patient was prevented for a long time with the use of tranilast for allergic rhinitis. Tranilast was originally developed as an anti-allergic drug for systemic or topical treatment of bronchial asthma, atopic dermatitis, and allergic conjunctivitis. Its usefulness in such applications is derived from its pharmacological ability to inhibit the release of chemical mediators from mast cells and to consequently suppress hypersensitivity reaction. Tranilast was also found to inhibit TGF-β production from human monocytes and macrophages, TGF-β expression in rat stellate cells, and TGF-β-induced collagen synthesis by keloid fibroblasts [15]. Furthermore, tranilast has been shown to have only minor clinical toxicity, such as cystitis and hepatitis, and no serious toxicity such as myelosuppression. Recently, several investigators reported anti-tumor effects of tranilast through different mechanisms. Shime et al. [16] reported that tranilast inhibited the proliferation of uterine leiomyoma cells in vitro through G1 arrest associated with the induction of p21 and p53. Nie et al. [17] reported that tranilast inhibited the insulin-like growth factor-1 (IGF-1)-induced cell growth in MCF-1 breast cancer cells by blocking calcium entry. Tranilast also inhibited cancer cell growth by suppressing intercellular interaction between cancer cells and stromal fibroblast in OCUM-2M gastric cancer cells and OSC-19 oral cancer cells [18,19]. However, there have been no reports about anti-tumor effects of tranilast on prostate cancer cells or clinical reports on any cancer cells. Therefore, anti-tumor effects of tranilast on prostate cancer cells should also be examined in both basic and clinical studies.

Based on these observations, we hypothesized that tranilast may cause apoptosis and cell cycle arrest of prostate cancer cells and inhibit production of TGF-β1 by osteoblasts and bone stromal cells, such as fibroblasts, in bone metastases. In the present study, we confirmed the effects of tranilast on prostate cancer cells and on inhibition of TGF-β1 production from bone stromal cells. In addition, we evaluated the effectiveness of tranilast in patients with advanced HRPC as a preliminary study.

MATERIALS AND METHODS

Chemicals

Tranilast (*N*-3,4-dimethoxycinnamoyl-anthranilic acid) was obtained from Kissei Pharmaceutical Co., Ltd. (Matsumoto, Japan). Tranilast was dissolved in dimethyl sulfoxide (DMSO; Sigma–Aldrich, St. Louis, MO) for the in vitro studies and in 0.5% carboxymethyl cellulose sodium salt (CMC; Wako, Osaka, Japan) solution for the in vivo studies.

Cell Line and Culture

Human SaOS-2 osteosarcoma cells (European Collection of Cell Cultures, Salisbury, UK) and PC-3 cells (American Type Culture Collection, Manassas, VA) were cultured in RPMI supplemented with 1% penicillin/streptomycin (Invitrogen, Carlsbad, CA) and 5% fetal bovine serum (FBS; Sigma–Aldrich). LNCaP parental cells (American Type Culture Collection) were cultured in DMEM supplemented with 1% penicillin/streptomycin and 5% FBS. An androgen-independent LNCaP cell line (LNCaP-SF), which was established in our laboratory after long-term subculture of the parental LNCaP cells in DMEM and 5% charcoal-stripped FBS (CCS; Hyclone, Logan, UT), was also used [20]. Bone-derived stromal cells 1 (BDSC-1) were obtained from the 11th rib of a 48-year-old Japanese man during left adrenalectomy for pheochromocytoma. Bone-derived stromal cells 2 (BDSC-2) were obtained from the 11th rib of a 58-year-old Japanese man during left nephroureterectomy for ureteral cancer without metastasis. Bone metastasis stromal cells (BmetSC) were obtained from the left thigh bone of

a 66-year-old Japanese man during palliative curettage for the pain of metastatic prostate cancer. We obtained informed consent for use of all specimens for experiments before each operation. These bone samples were scraped into bone chips and further processed with a bone grinder. Bone chips were cultured in RPMI supplemented with 1% penicillin/streptomycin and 10% FBS [21]. Normal human prostate stromal cells (PrSC; Cambrex, East Rutherford, NJ) were cultured using SCGM Bullet Kit (Cambrex). Each cell line was maintained at 37°C in a humidified atmosphere with 5% CO_2.

Animal Study

Severe combined immunodeficient (SCID) mice were castrated 1 week before implantation of LNCaP-SF cells. LNCaP-SF cells were combined with 50% Matrigel (Collaborative Biomedical Products, Bedford, MA) and 1×10^6 or 5×10^5 cells were prepared for injection into the dorsal subcutis or the left tibia of anesthetized (pentobarbital at 50 mg/kg body weight i.p.) 5-week-old castrated male SCID mice, respectively. Intratibial injection was performed using a 29-gauge, 0.5-in. needle inserted through the tibial plateau of the flexed knee as described previously [22]. Four weeks after inoculation, the dorsal tumor volume reached $142 \pm 134\,mm^3$, and mice were divided into three groups so that mean volume of each group became the same. The mice were then treated orally for 14 days with vehicle (control) or 100 or 200 mg/kg/day of tranilast in 5% CMC. Body weight was monitored at weekly intervals. Mice injected subcutaneously with LNCaP-SF cells were sacrificed 14 days following the start of oral administration of tranilast or vehicle alone. The tumor volume (V) was calculated from the length (l) and width (w) according to the formula $V = lw^2/2$. For mice receiving intratibial injections, 300 mg/kg/day of tranilast in 5% CMC solution or 5% CMC solution as a control was administered orally for 14 days from 12 weeks after injection. Mice injected into the left tibia were sacrificed at 14 weeks following intratibial injection. This protocol was approved by the Institutional Animal Care and Use Committee of the Graduate School of Medical Science, Kanazawa University.

Cell Proliferation

PC-3 and SaOS-2 cells were plated at a density of 5×10^4 cells onto six-well plates with RPMI 5% CCS and LNCaP, and LNCaP-SF cells were plated at a density of 1×10^5 cells onto six-well plates with DMEM 5% CCS. They were allowed to adhere and proliferate for 24 hr. Subsequently, each cell line was starved with serum-free medium (RPMI or DMEM) in the TGF-β1 experiment. Cells were incubated with fresh medium containing various doses between 0 and 300 μmol/L of tranilast for 24, 48, and 72 hr in the tranilast experiment, or 0, 0.5, and 5 ng/mL of human TGF-β1 (R&D Systems, Minneapolis, MN) daily for 7 days for the TGF-β1 experiment. In each experiment, cells were harvested and cell number was counted in triplicate using a hemocytometer.

ReverseTranscription-PCR

Twenty-four hours after seeding of each prostate cancer cell line at 5×10^5 cells per 6-cm dish, tranilast was added (0–300 μmol/L) for 48 hr, and cells were harvested. Total RNA extraction from cell cultures was performed using an RNeasy Mini Kit (Qiagen, Hilden, Germany). Total RNA (1 μg) was subjected to reverse transcription using ThermoScript RT (Invitrogen). Reverse transcription-PCR (RT-PCR) was performed using TaKaRa Ex Taq Hot Start Version (Takara Bio, Shiga, Japan). The sense and anti-sense primers used and RT-PCR conditions are shown in Table I.

TABLE I. The Primers Used for RT-PCR Analysis

Gene		Sequence and annealing temp. (°C)		Cycles
GAPDH	Forward	5′-GAC CAC AGT CCA TGC CAT CA-3′	60	21
	Reverse	5′-TCC ACC ACC CTG TTG CTG TA-3′		
p53	Forward	5′-TCC TCT TGC AGC AGC CAG ACT GCC T-3′	65	28
	Reverse	5′-GGG CAA CTG ACC GTG CAA GTC ACA G-3′		
p21	Forward	5′-AGG AGG CCC GTG AGC GAT GGA ACT T-3′	65	28
	Reverse	5′-CTG TCA TGC TGG TCT GCC GCC GTT T-3′		
p27	Forward	5′-CTA GAG GGC AAG TAC GAG TGG CAA G-3′	65	32
	Reverse	5′-GAA GAA TCG TCG GTT GCA GGT CGC T-3′		
Osteopontin	Forward	5′-TAT GAT GGC CGA GGT GAT AGT GTG G-3′	65	30
	Reverse	5′-TAA TCT GGA CTG CTT GTG GCT GTG G-3′		
cbfa-1	Forward	5′-CCC ACG AAT GCA CTA TCC AGC CAC C-3′	65	30
	Reverse	5′-ATT CGA GGT GGT GGT GCA TGG CGG A-3′		

Western Blotting Analysis

Twenty-four hours after each prostate cancer cell line was seeded at 1×10^6 cells per 6-cm dish, tranilast was added (0–300 μmol/L) for 48 hr. Cells were harvested, washed with PBS, and lysed using radioimmunoprecipitation assay buffer (50 mmol/L Tris–HCl, pH 8.0, 150 mmol/L NaCl, 0.1% Triton X-100, 0.01 mg/mL aprotinin, 0.05 mg/mL phenylmethylsulfonyl fluoride). The nuclei and cellular debris were removed by centrifugation at 12,000*g* for 10 min at 4°C. Protein was quantified according to the method of Bradford, and equal amounts of protein were loaded and electrophoresed on a 10% or 12.5% sodium dodecyl sulfate–polyacrylamide gel. Proteins in the gel were transferred onto polyvinylidene difluoride membranes (Bio-Rad, Hercules, CA) and pre-blocked with casein PBS and 0.05% Tween-20 for 1 hr at room temperature. Membranes were incubated with mouse monoclonal antibody against p53, p27, and full-length poly (ADP-ribose) polymerase (PARP), and rabbit polyclonal antibody against p21, Fas (Santa Cruz Biotechnology, Santa Cruz, CA), and cleaved PARP (Abcom, Cambridge, MA). Horseradish peroxidase-conjugated secondary antibody against anti-mouse monoclonal or anti-rabbit monoclonal or polyclonal antibody was used and protein bands were visualized with enhanced chemiluminescence reagent (SuperSignal West Pico Chemiluminescent Substrate; Pierce, Rockford, IL). Equal loading of proteins was confirmed using Ponceau S solution (Sigma–Aldrich).

Cell Cycle Analysis

Twenty-four hours after each prostate cancer cell line was seeded at 1×10^6 cells per 6-cm dish, tranilast was added (0–300 μmol/L) for 48 hr. Cells were then harvested, washed with PBS, and fixed in 100% ethanol for 30 min at −20°C. They were then treated with 5 μg/mL of RNase for 30 min, stained with 50 μg/mL propidium iodide, and analyzed by flow cytometry for cell cycle status (Beckman–Coulter, Fullerton, CA).

Apoptosis Assay

Twenty-four hours after each prostate cancer cell line was seeded at 5×10^4 cells per six-well plate, tranilast was added (0 or 300 μmol/L) for 48 hr. The terminal deoxynucleotidyl transferase-mediated dUTP-biotin nick end-labeling (TUNEL) technique was used to detect apoptotic cells using an in situ Apoptosis Detection Kit (Takara Bio) in accordance with the manufacturer's instructions. Optical microscopy was performed to confirm the existence of positively stained cells.

Coculture of SaOS-2 or Bone-Derived Stromal Cells With LNCaP-SF

Aliquots of 5×10^4 SaOS-2, BDSC-1, BDSC-2, or BmetSC cells were plated onto Cell Culture Inserts (1.0 μm pore size 12-well format; Becton–Dickinson, Franklin Lakes, NJ) with RPMI 10% FBS in 12-well plates containing RPMI 10% FBS for 24 hr. Each cell line was starved with serum-free DMEM and applied to 12-well plates containing cultures of LNCaP-SF cells as follows. LNCaP-SF cells were plated at a density of 5×10^4 cells onto 12-well plates with DMEM 5% CCS. After cells were allowed to adhere and proliferate for 24 hr, they were starved with serum-free DMEM. Then, each Cell Culture Insert including BDSC or SaOS-2 was placed on these 12-well plates. After 7 days, LNCaP-SF cells were harvested and cell number was counted in triplicate using a hemocytometer.

Morphological Transformation of Bone-Derived Stromal Cells by TGF-β1

After aliquots of 5×10^4 BDSC-1, BDSC-2, or BmetSC cells were plated onto 12-well plates with RPMI 10% FBS, they were allowed to adhere and proliferate for 24 hr. Subsequently, each cell line was starved with serum-free RPMI. Cells were incubated with fresh medium containing various doses between 0, 0.5, and 5 ng/mL TGF-β1 and 0.5 ng/mL TGF-β1 with 10 μg/mL of pan-specific TGF-β antibody (R&D Systems) daily or 0.5 ng/mL of TGF-β1 daily with 0–300 μmol/L of tranilast every other day for 10 days. In each experiment, cells were observed morphologically and the cellular area of each of 20 cells was determined using NIH image[1] to express the changes as objective values. Cells were subsequently harvested and cell number was counted in triplicate using a hemocytometer. Total RNA extraction and RT-PCR were performed as described above.

Enzyme-Linked Immunoassay (ELISA)

After 2×10^5 PC-3, LNCaP, LNCaP-SF, or SaOS-2 cells and 1×10^5 BDSC-1, BDSC-2, or BmetSC cells were plated onto six-well plates with RPMI 5% CCS or DMEM 5% CCS, cells were treated with 0–300 μmol/L tranilast for 48 hr. Culture medium was harvested and centrifuged to remove debris. Samples were stored at −80°C until use. TGF-β1 protein secretion was determined using Quantikine Human TGF-β1 (R&D Systems) according to the manufacturer's instructions. In each experiment, cells were harvested and cell number was counted in triplicate using a hemocytometer.

[1]This has been detailed at http://rsb.info.nih.gov/nih-image/.

Values are expressed as secreted TGF-β1 pg/ml/1×10^5 cells.

Wound Assay

The post-confluent LNCaP-SF cells were used in this experiment. Wounds with a constant diameter were made. Cells were treated with recombinant human osteopontin (R&D Systems) alone or with tranilast in 5% CCS or serum free medium. The wound photographs were taken and the distance between the wound edges was measured at 0 and 96 hr.

Patients

Sixteen patients with HRPC who had received several salvage therapies that had not been effective were orally administered tranilast at a dose of 300 mg/day at Kanazawa University Hospital and associated institutions. Before starting tranilast treatment, we confirmed that PSA level continuously increased more than three times despite one or more salvage therapies. We did not start other new or alternative treatments. However, in cases in which other treatments were performed during tranilast treatment, this clinical study was terminated. PSA was examined once in a month. Stable disease was defined as the condition in which PSA level was lower than that when tranilast was started. All studies were performed after receiving approval from the Institutional Review Board of the Graduate School of Medical Science, Kanazawa University, and after the subjects gave their informed consent to participation in the study.

Statistical Analysis

Student's *t*-test was used to determine the statistical significance of differences in results of proliferation assay, cellular area, and ELISA between the control and others and differences in subcutaneous tumor size between the control and treated groups in vivo. The χ^2 test was used to determine the significance of differences of radiographic changes between treated and control groups in vivo. $P < 0.05$ was considered statistically significant.

RESULTS

Tranilast Inhibits Tumor Growth of LNCaP-SF Cells Inoculated Into the Dorsal Subcutis and the Tibia

To explore the mechanism of the anti-tumor effect of tranilast, we initially examined the direct effect of tranilast on prostate cancer cell growth. Tranilast diminished cell numbers of LNCaP, LNCaP-SF, and PC-3 cells in a dose-dependent manner (Fig. 1A).

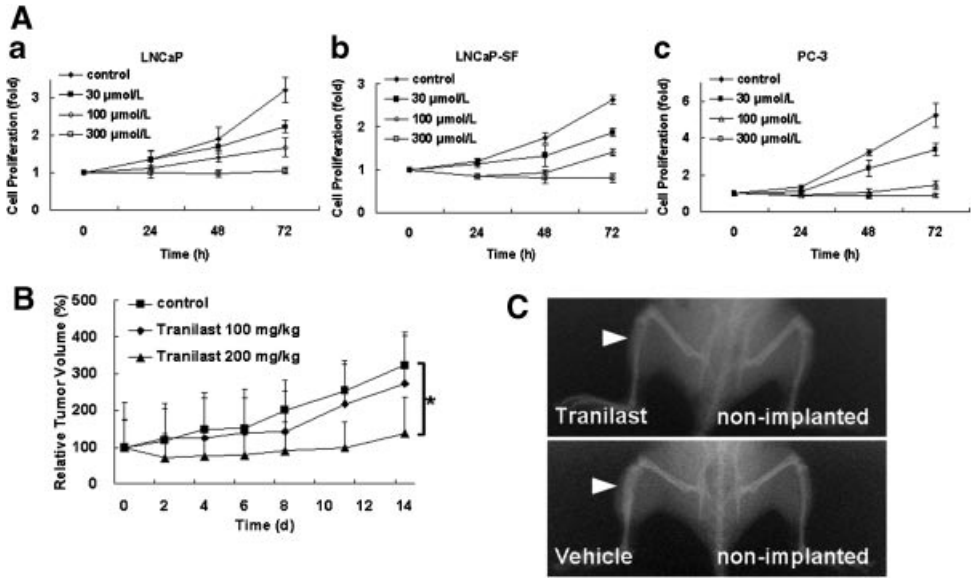

Fig. 1. **A**: Tranilast decreases proliferation of LNCaP, LNCaP-SF, and PC-3 cells in vitro. LNCaP, LNCaP-SF, and PC-3 cells were treated with tranilast (0–300 μmol/L) as described in Materials and Methods Section. After 24 hr of exposure, ≥100 μmol/L tranilast caused significant inhibition in LNCaP-SF and PC-3 cells. After 72 hr of exposure, ≥30 μmol/L tranilast caused significant inhibition in all cell lines ($P < 0.05$–0.001). Points, mean ratio to control (n = 3); bars, SD. **B**: Four weeks after inoculation of LNCaP-SF cells, the dorsal tumor volume reached 100–200 mm^3, and mice were divided into three groups so that mean volume of each group become same. The mice were then treated orally daily for 14 days with vehicle (control) or 100 or 200 mg/kg/day of tranilast (*$P = 0.048$). Points, mean percent of control (n = 6 per group); bars, SE. **C**: For mice that received intratibial injection of LNCaP-SF cells, vehicle (control) or 300 mg/kg/day of tranilast was administered orally for 14 days from 12 weeks after injection. Mice were sacrificed at 14 weeks following intratibial injection. Representative radiographs of intact tibia in the tranilast-treated mice and osteoblastic changes in vehicle-treated controls are shown (n = 9 per group).

To confirm the effect of tranilast on tumor growth in vivo, we inoculated LNCaP-SF into the dorsal subcutis of SCID mice and treated mice with oral administration of tranilast. Tranilast at 200 mg/kg/day significantly reduced tumor volume to 50% of that in the control group at 2 weeks after tranilast administration ($P = 0.048$, Fig. 1B).

Next, as a model of osteoblastic metastasis, we used LNCaP-SF cells for in vivo study because these cells induced osteoblastic changes when inoculated into the tibia of castrated male mice [20]. Vehicle and tranilast at 300 mg/kg/day were administered orally ($n = 9$ per group). Radiographic evidence of osteoblastic lesions was observed in eight of nine (88.9%) mice in the control group. Whereas tranilast at 300 mg/kg/day significantly inhibited osteoblastic changes in three of nine (33.3%) mice ($P = 0.016$, Fig. 1C). No differences were observed in body weight between the vehicle-treated group and the tranilast-treated group (data not shown).

Tranilast Induces Cell Cycle Arrest Associated With Induction of p53, p21, and p27, and Causes Apoptosis

Flow cytometric analysis revealed that tranilast increased the distribution of cells remaining at G1 phase in LNCaP and LNCaP-SF cells in a dose-dependent manner (Fig. 2A). Moreover, tranilast increased the distribution of cells remaining at S phase along with G1 phase increased in PC-3 cells in a dose-dependent manner. Tranilast increased the levels of p53, p21, and p27 mRNA and protein expression in LNCaP and LNCaP-SF cells (Fig. 2B). In PC-3 cells, which originally do not express p53, tranilast increased the levels of p21 mRNA and protein expression but not that of p27 mRNA. To further investigate whether the anti-growth effect of tranilast is also associated with apoptosis, we performed TUNEL assay. Nuclear fragmentation, a typical morphological hallmark of apoptosis, was observed following treatment with 300 μmol/L tranilast in LNCaP, LNCaP-SF, and PC-3 cells (Fig. 2C). Tranilast increased Fas and cleaved product of PARP, and diminished full-length PARP in LNCaP, LNCaP-SF, and PC-3 cells in a dose-dependent manner (Fig. 2D).

Roles of SaOS-2 or Bone-Derived Stromal Cells on LNCaP-SF

Since tranilast inhibited both tumor growth on the dorsal subcutis of SCID mice osteoblastic changes induced by LNCaP-SF in the tibia of SCID mice, we explored for other potential mechanisms of the inhibition of the osteoblastic changes caused by tranilast, and focused on how tranilast affects TGF-β1 function.

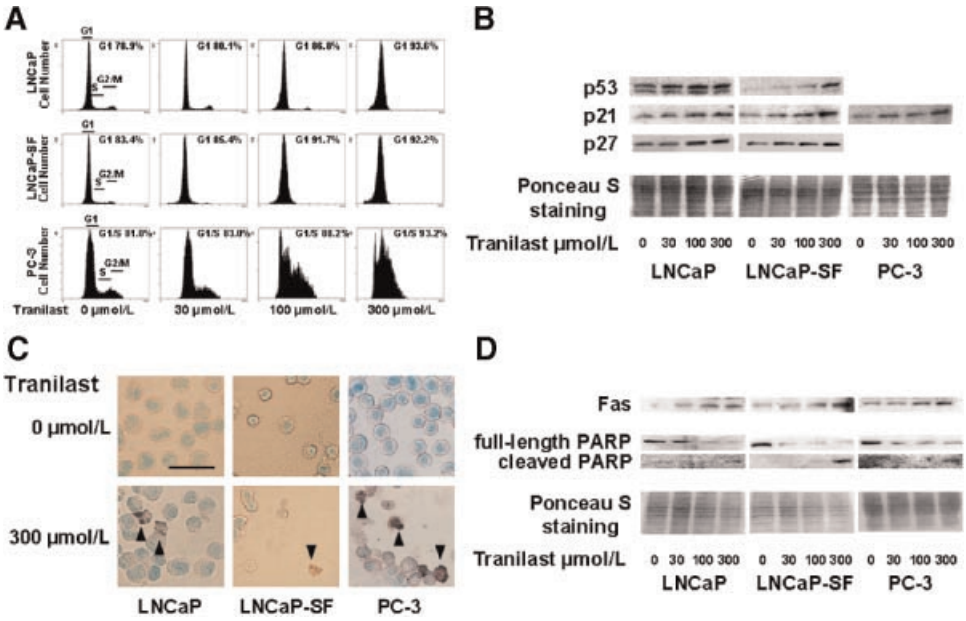

Fig. 2. Tranilast induces cell cycle arrest and apoptosis in LNCaP, LNCaP-SF, and PC-3 cells. **A**: Cell cycle analysis was performed with flow cytometry as described in Materials and Methods Section. Each panel shows representative results from one of the three experiments. **B**: Western blotting analyses of cell-cycle-related genes were performed. Twenty-four hours after each prostate cancer cell line was seeded at 1×10^6 cells per 6-cm dish, tranilast was added (0–300 μmol/L) for 48 hr, and each cell line was harvested. **C**: Cells were treated with 0 or 300 μmol/L tranilast for 48 hr and TUNEL assay was performed. The existence of positively stained cells with nuclear fragmentation was confirmed by optical microscopy. Arrowheads indicate apoptotic cells. Bar, 100 μm. **D**: Western blotting analysis of Fas (48 kDa), full-length PARP (112 kDa), and proteolytic cleavage of PARP (85 kDa), which are apoptosis-related genes.

First, we established primary cultures of bone-derived stromal cells, BDSC-1, BDSC-2, and BmetSC. To confirm that BDSC-1, BDSC-2, and BmetSC were stromal cells derived from bone tissue, we examined the expression of the osteoblastic markers osteopontin and cbfa-1 by RT-PCR [23]. Osteopontin mRNA expression was observed in BDSC-1, -2, and BmetSC, but not in PrSC, although cbfa-1 mRNA expression was exhibited in all types of stromal cells examined (data not shown). To seek evidence for the ability of TGF-β1 production at the bone metastatic site to induce proliferation of prostate cancer cells, we cocultured SaOS-2 and BDSC, which produce high levels of TGF-β1, with LNCaP-SF cells. As shown in Figure 3A, coculture with SaOS-2 and BDSC strongly induced proliferation of LNCaP-SF cells. These results indicate that stromal cells can promote prostate cancer proliferation at the osteoblastic metastatic site. However, they do not prove that this occurs through TGF-β1.

To determine if TGF-β1 produced by the stromal cells could mediate the proliferative affect, we grew prostate cancer cells and osteoblast-like cells in the presence of TGF-β1. TGF-β1 did not induce any changes in proliferation of LNCaP, LNCaP-SF, or PC-3 cells (data not shown) indicating that the stromal cells did not induce prostate cancer proliferation through TGF-β1.

TGF-β1 Induces Differentiation of Bone-Derived Stromal Cells

To determine if TGF-β1 impacted the osteoblastic nature of the stromal cells in the osteoblastic metastatic site, we cultured the stromal and SaOS-2 cells with TGF-β1. Similar to the prostate cancer cell lines, TGF-β1 did not induce proliferation of SaOS-2, BDSC-1, BDSC-2, and BmetSC (data not shown); however, it did induce morphological transformation into polygonal cells and marked increases in size (Fig. 3B, a–d). To express this change as an objective value, we quantified the cellular area in cultures treated with 0, 0.5, and 5 ng/ml of TGF-β1 and 0.5 ng/ml of TGF-β1 with 10 μg/ml of pan-specific TGF-β antibody using NIH image. TGF-β1 increased the cellular area by 6.2- and 5.6-fold as compared with controls as in 0.5 and 5 ng/ml in BDSC-1, 12.2- and 7.9-fold in BDSC-2, and 3.2- and 3.5-fold in BmetSC. This effect was inhibited by addition of pan-specific TGF-β1 antibody (Fig. 3B, left). To determine whether TGF-β1 induced osteogenic differentiation of BDSC, we examined the changes in osteopontin and cbfa-1 mRNA levels by RT-PCR. The expression level of osteopontin mRNA was increased by 0.5 and 5 ng/ml of TGF-β1 and inhibited by pan-specific TGF-β1 antibody (Fig. 3B, right). These results indicated that TGF-β1 promotes differentiation of BDSC at a low concentration.

As TGF-β1 induced differentiation of BDSC, we investigated if tranilast could impact this differentiation. Morphological change induced by 0.5 ng/ml TGF-β1 was inhibited in all BDSC by tranilast in a dose-dependent manner (Fig. 3C, a–d). Tranilast decreased the cellular area by 0.63- and 0.19-fold as compared with 0 μmol/L at 100 and 300 μmol/L in BDSC-1, 0.49- and 0.15-fold in BDSC-2, and 0.54- and 0.12-fold in BmetSC (Fig. 3C, left). Furthermore, ≥100 μmol/L of tranilast repressed the expression level of osteopontin mRNA induced by 0.5 ng/ml TGF-β1 (Fig. 3C, right).

Tranilast Inhibits TGF-β1 Production From Bone-Related Cells

To evaluate the effects of tranilast on TGF-β1 production from SaOS-2, BDSC-1, BDSC-2, and BmetSC (bone-related cells), we measured secreted TGF-β1 protein level in the culture medium on cells treated with 0–300 μmol/L tranilast. Although PC-3 cells secreted TGF-β1 (<290 pg/ml at most), LNCaP and LNCaP-SF cells hardly secreted TGF-β1. Tranilast did not alter the secretion of TGF-β1 from these cell lines. In contrast, bone-related cells secreted TGF-β1 in the range of 600–1,100 pg/ml. Tranilast decreased TGF-β1 secretion from these bone-related cells in a dose-dependent manner. Especially, tranilast caused significant inhibition at concentrations of ≥30 μmol/L in BDSC-1 and BDSC-2, ≥100 μmol/L in SaOS-2, and 300 μmol/L in BmetSC (Fig. 4A).

Osteopontin Promotes Migration of LNCaP Cells

To study the role of osteopontin in tumor migration, we examined its ability to stimulate LNCaP-SF cell migration in a wound assay (Fig. 4B). Because LNCaP-SF cells formed osteoblastic lesion similar to typical prostate cancer bone metastasis, we employed LNCaP-SF cells for this experiment. Whereas LNCaP-SF cells in 5% CCS medium did not change migration rate even if they were stimulated by osteopontin, LNCaP-SF cells in serum-free medium with osteopontin had a significantly higher migration rate compared with control. The migration rate of LNCaP-SF was significantly decreased by tranilast in both 5% CCS and serum-free medium (Fig. 4C).

PSA Progression of Patients With Advanced HRPC Is Suppressed by Tranilast

Our in vitro and murine model data suggested that tranilast may have an impact on prostate cancer growth. Accordingly, we performed a small clinical evaluation of tranilast in patients with the goal of

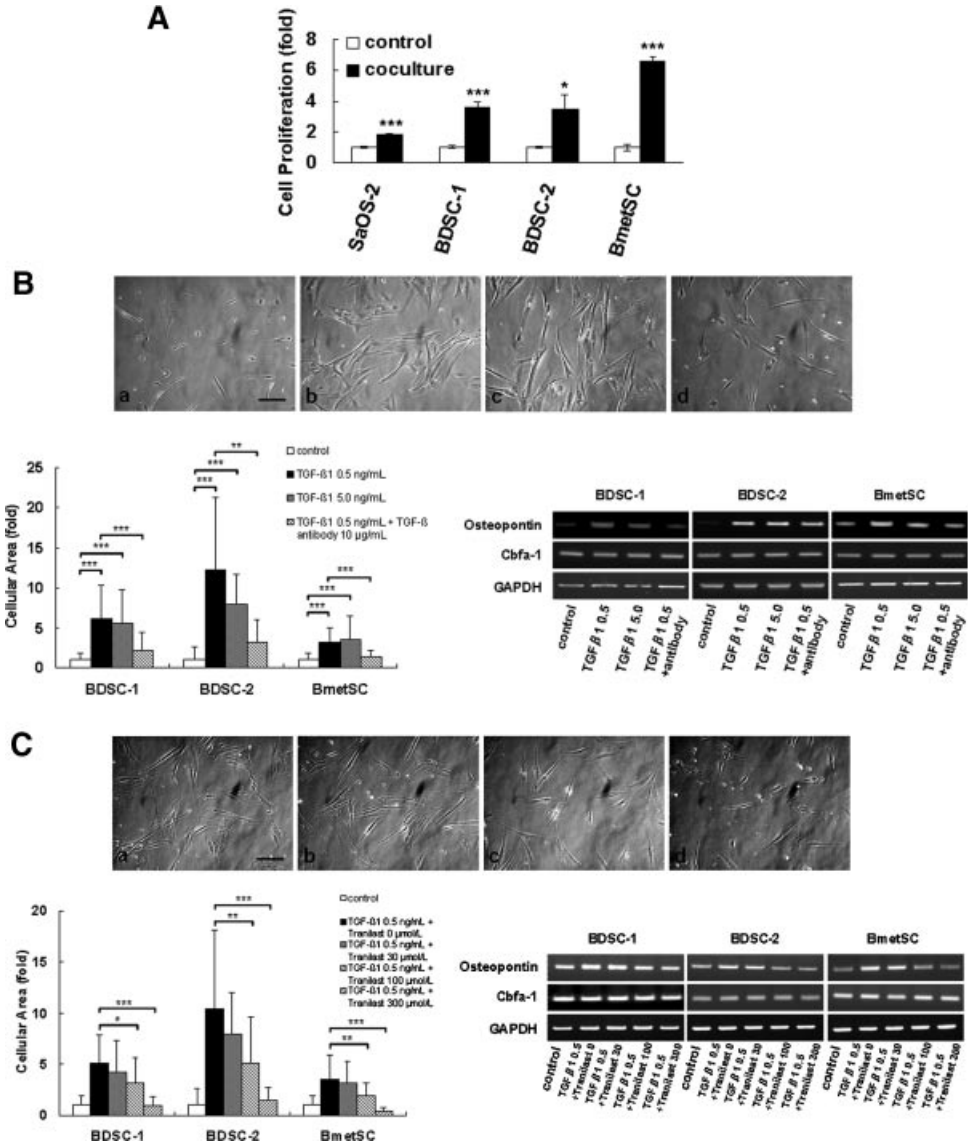

Fig. 3. Effects of TGF-β1 and/or tranilast on bone-derived stromal cells. **A**: Coculture of LNCaP-SF with SaOS-2 or bone-derived stromal cells was performed as described in Materials and Methods Section. Bars, SD. **B**: Morphological transformations in BDSC-2 growing as representatives of bone-derived stromal cells were determined by phase-contrast microscopy. Bar, 200 μm. Cells were incubated with various concentrations between 0 (control) (**a**), 0.5 (**b**), and 5 (**c**) ng/ml of TGF-β1 and 0.5 ng/ml of TGF-β1 with 10 μg/ml of pan-specificTGF-β antibody (**d**) daily for 10 days. As a sign of cellular differentiation, cellular areas were gauged and quantified by NIH image to express the changes with objective values (left). To examine osteogenic differentiation, mRNA levels of osteopontin and cbfa-1 were also examined by RT-PCR (right). **C**: Morphological transformations in BDSC-2 growing as representatives of bone-derived stromal cells were determined by phase-contrast microscopy. Cells were incubated with 0.5 ng/ml of TGF-β1 daily and varying concentrations of tranilast between 0 (**a**), 30 (**b**), 100 (**c**), and 300 (**d**) μmol/L every other day for 10 days. Cellular areas were gauged and quantified (left), and mRNA levels of osteopontin and cbfa-1 were also examined by RT-PCR (right) (*$P < 0.05$, **$P < 0.01$, ***$P < 0.001$).

determining if tranilast would warrant a full clinical trial. Table II lists baseline clinical characteristics of 16 patients with advanced HRPC. Six patients had both bone metastases and lymph node metastases and eight patients had bone metastases alone. Two patients had local extra-prostate invasion of ≥T3 with no evidence of metastasis. All patients had been treated with combined androgen blockade (CAB) and followed by one or more salvage therapies, nevertheless, their PSA continued to increase at least three times before starting tranilast. As shown in Figure 5, after commencement of tranilast administration, PSA progression was inhibited in four (25%) patients (for 13, 1, 10, and 3 months, respectively). There were no differences in clinical characteristics between cases in which tranilast was and was not effective; however, all patients who

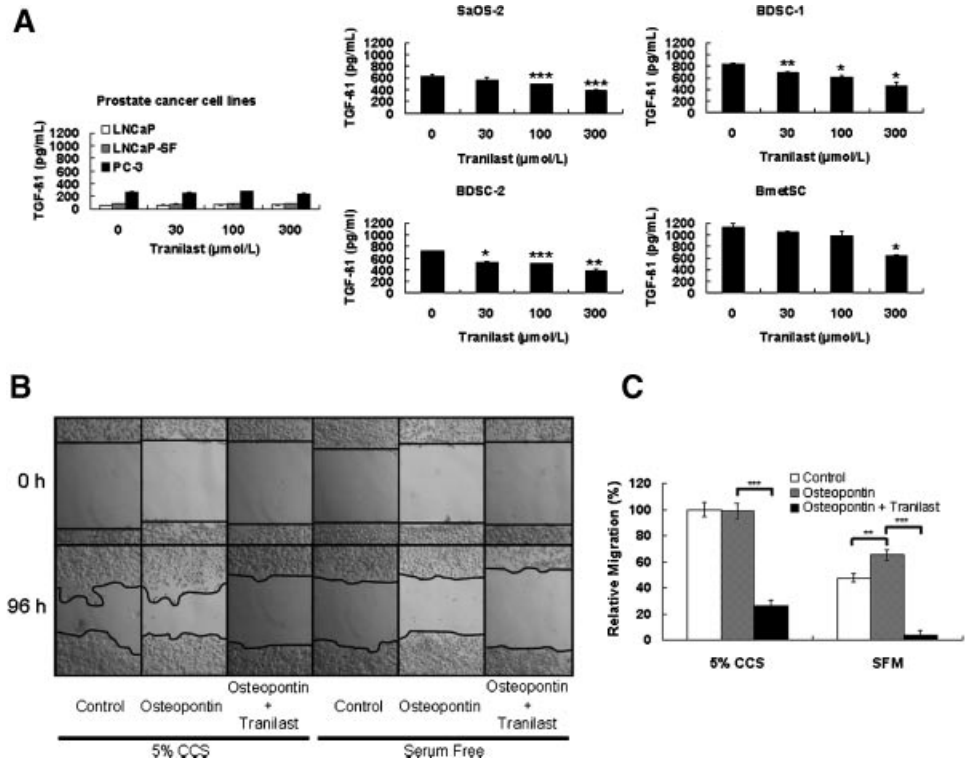

Fig. 4. **A**: The changes in TGF-β1 secretion in prostate cancer cell lines, SaOS-2, and bone-derived stromal cells by tranilast were examined by ELISA as described in Materials and Methods Section. Bars, SD. **B**: Osteopontin (1 μg/ml) was added daily and 300 μmol/L tranilast was added every other day to LNCaP-SF cells. Wound photographs were taken under phase-contrast microscopy at initial time (0 hr) and the termination of the experiments (96 hr). **C**: Results are presented as the percentage to control in 5%CCS (*$P < 0.05$, **$P < 0.01$, ***$P < 0.001$).

responded to tranilast had bone metastasis. Adverse events were observed in two cases; elevation of liver enzymes and headache in one case. Each adverse event was improved rapidly after withdrawal of tranilast.

DISCUSSION

Tranilast, which is used as oral medicine for the treatment of allergic diseases in Japan, showed an inhibitory effect on proliferation of prostate cancer cells both in vitro and in vivo. Moreover, our preliminary clinical trial suggested that tranilast may be effective in a subset of patients with HRPC without severe side effects.

Flow cytometric analysis indicated that tranilast arrested the cell cycle of LNCaP and LNCaP-SF cells in the G1 phase. Cyclin-dependent kinases (CDKs) play a central role in the cell cycle of mammalian cells and promote G1/S transition by phosphorylation of the retinoblastoma protein [24]. Intrinsic CDK inhibitors, such as p21 and p27, bind to the CDK–cyclin complex and inhibit its kinase activity, and p53 is a well-known cellular transcription factor that stimulates the expression of various genes, including p21 [24,25]. We clarified that tranilast up-regulated the levels of p53, p21, and p27 expression in LNCaP and LNCaP-SF in a dose-dependent manner. It was reported that tranilast induced expression of p21 and p53 as well as G1 arrest, and decreased CDK2 activity in uterine leiomyoma cells and human malignant glioma cells [16,26]. Consistent with these reports, our results suggested that tranilast induced G1 arrest in LNCaP and LNCaP-SF cells via induction of p53, p21, and p27. On the other hand, PC-3 cells, which have a mutation in p53 [27], did not show changes in p27 expression and increased p21 expression, and accumulated in not only G1 phase but also S phase. S phase checkpoints play critical roles in maintaining genomic integrity and correct replication of the genomic DNA. It was reported that apoptosis is regulated through an S phase checkpoint controlled by the checkpoint kinase (Chk)1-Cdc25A and Chk2-Cdc25A pathways in C4-2 human prostate cancer cell line which is androgen-independent and express low levels of p53 [28]. Effects of tranilast on the cell cycle in PC-3 cells may be different from those in LNCaP and LNCaP-SF cells.

Moreover, apoptosis induced by tranilast was confirmed based on the nuclear morphological changes determined by TUNEL assay, and the levels of expression of the apoptosis-related proteins Fas and cleaved PARP were increased by tranilast. Up-regulation of Fas occurs in tumor cells following

TABLE II. Characteristics of 16 Patients With Advanced HRPC

Median age at diagnosis (range)	66.5 (57–88)
Median PSA ng/mL at diagnosis (range)	200 (4.8–4,370)
Median PSA ng/ml at starting tranilast (range)	25.8 (0.99–2,079)
Median months from diagnosis to starting tranilast (range)	42 (12–89)
Median months follow-up (range)	3 (1–19)
Gleason's score	
<7	2
=7	8
>7	6
T stage	
T1–2	3
T3–4	13
Metastasis	
No. of lymph nodes	6
No. of bone	14
Previous treatment	
Radical prostatectomy	1
Castration	16
Anti-androgen	16
Estramustine phosphate	14
Dexamethasone	7
Bisphosphonate	6
Chemotherapy	3
Radiation	2

Castration included one case of surgical castration, while the others were medical castrations.

chemotherapy and may play a key role in evasion of immune surveillance by eliminating infiltrating lymphocytes [29]. Thus, tranilast directly inhibits prostate cancer cell proliferation by inducing cell cycle arrest and apoptosis.

In the present study, the anti-tumor effect of tranilast on LNCaP-SF xenografts was observed not only in those injected subcutaneously but also in those with direct tibial injection of castrated male SCID mice. The extracellular bone matrix proteins of osteoblastic lesions are known to enhance proliferation and differentiation of prostate cancer cells in vivo and do so in many culture systems. It was reported that osteoblast-conditioned medium increased the proliferation and expression of PSA at both the protein and mRNA levels in LNCaP cells [30]. In addition, bone fibroblasts differentially modulated LNCaP growth through the release of paracrine-mediated growth factors [31]. We also found that coculture of LNCaP-SF cells with bone-related cells induced proliferation of LNCaP-SF cells. Moreover, bone-related cells secreted higher levels of TGF-β1 than prostate cancer cells, which tranilast targets. However, our results showing that TGF-β1 did not directly stimulate prostate cancer cell growth suggest that tranilast does not achieve its affects through blocking a proliferative effect induced by TGF-β1 on prostate cancer cells.

Among the cytokines in osteoblastic metastasis, TGF-β requires activation from its precursor form, which can be catalyzed by PSA, and plays an important role in skeletal remodeling [32]. Kassem et al. [33] reported that TGF-β1 increased osteoblastic cell proliferation irrespective of their differentiation state. Osteopontin, one of the most prevalent non-collagenous proteins secreted by osteoblasts accumulates in the mineralized extracellular matrix and is involved in bone remodeling and signaling [34]. Frank et al. [35] also reported that the level of osteopontin mRNA can be used as a marker to monitor the extent of bone stromal cell osteogenic differentiation in vitro. Osteopontin has also been implicated tumor invasion and metastasis in prostate and other cancers. In the present study, even a low concentration of TGF-β1 (0.5 ng/ml) led BDSC to morphological transformation, increases in size, and up-regulation of osteopontin mRNA. In addition, osteopontin promoted LNCaP-SF cell migration. Taken together, these results suggested that TGF-β1 may accelerate differentiation and its effects in cells of the osteoblast lineage in an autocrine manner and that tumor–stromal cell interaction plays an important role in prostate cancer growth and progression in bone.

Platten et al. [26] and Yashiro et al. [36] also reported that tranilast inhibited the release of TGF-β1 and -β2 from human malignant glioma cells and from gastric fibroblasts. In the present study, we showed that tranilast diminished TGF-β1 secretion from bone-related cells in a dose-dependent manner, but not from LNCaP, LNCaP-SF, or PC-3. Moreover, the differentiation effects of TGF-β1 on BDSC were also inhibited by tranilast in a dose-dependent manner. Tranilast may not only directly inhibit the proliferation of prostate cancer cells but also indirectly suppress TGF-β1-associated osteoblast differentiation and proliferation, and prostate cancer proliferation and migration via inhibiting TGF-β1 and osteopontin secretion from osteoblasts and stromal cells (Fig. 6).

The clinical study in this article is the first pilot trial of tranilast use for treatment of patients with cancer. PSA is a very sensitive, specific, and meaningful serum marker for tumors of prostate origin in all clinical situations and is correlated to clinical condition [37]. Generally, once prostate cancer becomes advanced HRPC after several rounds of salvage therapy, the general condition of the patient becomes worse with continuous PSA progression without temporary recovery. Our data showed that 4 of 16 patients with advanced HRPC responded to oral 300 mg/day tranilast administration with respect to PSA. Clinically,

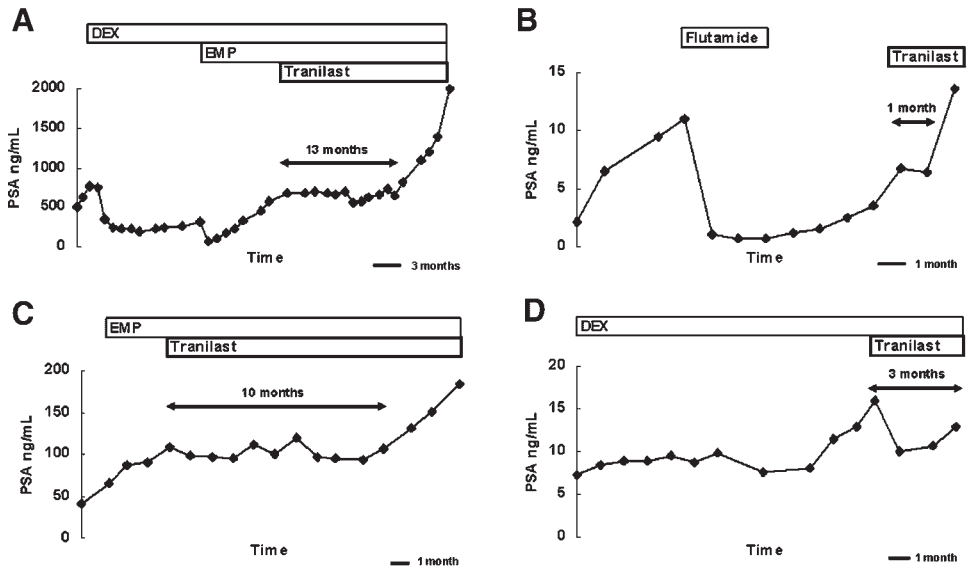

Fig. 5. Cases in which tranilast treatment was effective. **A**: An 80-year-old patient who had received CAB, alternative anti-androgens, EMP, DEX, tegafur uracil, and incadronate as previous treatments maintained stable disease for 13 months. This patient died from prostate cancer 19 months after starting tranilast. **B**: A 79-year-old patient treated previously with CAB and alternative anti-androgens maintained stable disease for only 1 month, but PSA decreased markedly after starting tranilast. **C**: A 57-year-old patient treated previously with CAB, EMP, and ethinylestradiol maintained stable disease for 10 months. **D**: An 80-year-old patient treated previously with CAB, alternative anti-androgens, EMP, and DEX maintained stable disease for 3 months. This patient's disease was still stable at the time of submission of this study. Parts of the clinical data of these patients are not shown because the duration from diagnosis to starting tranilast was very long in each case: 89, 28, 33, and 88 months, respectively.

tranilast functioned as a cytostatic rather than a cytotoxic agent. It was reported that the attainable serum concentration of tranilast reaches 30–300 μmol/L in vivo after oral administration of 600 mg/day tranilast [38]. The administered dose of tranilast may be too low to overcome multiple metastases. The results of the present study, however, suggested that tranilast may have beneficial effects on the inhibition of PSA progression in a subset of patients with HRPC. Although severe adverse events that result in discontinuation of treatment can often occur in chemotherapy and molecular targeting therapy, only two patients in the present study had minor adverse events.

In addition, it was reported that tranilast inhibited the IGF-1-induced cell growth in MCF-1 breast cancer cells by blocking calcium entry [17]. IGF-1 is also abundant in bone cortex and it was reported that IGF-1 plays a role as a risk factor in prostate cancer [39].

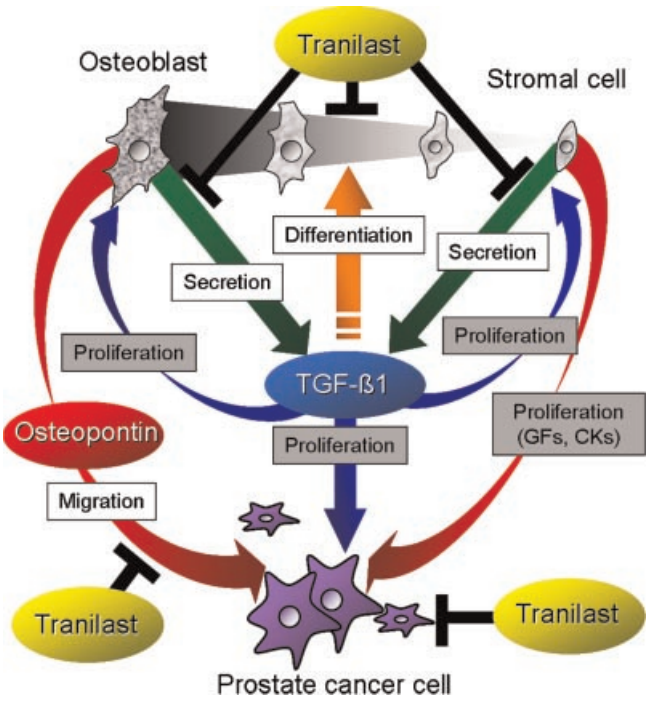

Fig. 6. Schematic illustration of the effects of TGF-β1 and tranilast. In site of bone metastases, osteoblasts and stromal cells initially secreted TGF-β1, which induces proliferation and self-differentiation, and subsequently they induce migration and proliferation of prostate cancer cells by releasing growth factors (GFs) or cytokines (CKs) such as osteopontin in a chain reaction. Tranilast directly inhibits prostate cancer cell proliferation via cell cycle arrest and induction of apoptosis. Tranilast also inhibits secretion of TGF-β1 from osteoblasts and stromal cells. Moreover, tranilast suppresses the effects of TGF-β1 on stromal cells. Accordingly, osteoblastic changes in bone metastatic site are inhibited. Although proliferation with gray rectangle mentioned in schema was not confirmed in this study; however, they were previously reported in some prostate cancer cell lines.

Tranilast may inhibit proliferation of prostate caner in bone metastasis meditated through suppression of IGF-1 secretion from the bone cortex as well as TGF-β1. Recently, Fan et al. [40] reported that tranilast may be able to enhance the anti-tumor effect of romidepsin (FK228, depsipeptide), a unique cyclic depsipeptide with a histone deacetylase inhibitor activity, in bladder cancer cells. Tranilast may also become a useful chemical agent for combination therapy with chemotherapy or molecular targeting therapy.

In conclusion, tranilast may be a useful new therapeutic agent that can prolong survival and improve the prognosis of HRPC patients. Tranilast may be worth trying in HRPC patients before chemotherapy because it is administered orally and has few side effects. Further studies are required to determine the mechanism by which tranilast inhibits TGF-β1 production of bone stromal cells and TGF-β1 acts on bone stromal cells and prostate cancer cells in bone metastasis, and to specify the subpopulation for which tranilast is effective. Moreover, as the study population here was small and it was performed as an open-label study with one arm, it is also necessary to assess larger numbers of HRPC patients.

ACKNOWLEDGMENTS

A Grant-in-Aid for Scientific Research on Priority Areas from the Ministry of Education, Culture, Sport, Science, and Technology of Japan and National Institutes of Health P01 CA093900. The costs of publication of this article were defrayed in part by the payment of page charges. This article must therefore be hereby marked advertisement in accordance with 18 U.S.C. Section 1734 solely to indicate this fact. We thank Tetsumori Yamashima (Department of Restorative Neurosurgery, Kanazawa University Graduate School of Medical Science) and Junko Sakaguchi (Department of Obstetrics and Gynecology, Kanazawa University Graduate School of Medical Science) for helpful suggestions regarding the use of flow cytometry.

REFERENCES

1. Jemal A, Siegel R, Ward E, Hao Y, Xu J, Murray T, Thun MJ. Cancer statistics, 2008. CA Cancer J Clin 2008;58:71–96.
2. Rubin MA, Putzi M, Mucci N, Smith DC, Wojno K, Korenchuk S, Pienta KJ. Rapid (''warm'') autopsy study for procurement of metastatic prostate cancer. Clin Cancer Res 2000;6:1038–1045.
3. Denis L. Prostate cancer. Primary hormonal treatment. Cancer 1993;71(3 Suppl.):1050–1058.
4. Petrylak DP. Chemotherapy for advanced hormone refractory prostate cancer. Urology 1999;54(6A Suppl.):30–35.
5. Oh WK. Chemotherapy for patients with advanced prostate carcinoma. A new option for therapy. Cancer 2000;88(12 Suppl.): 3015–3021.
6. Kojima S, Suzuki H, Akakura K, Shimbo M, Ichikawa T, Ito H. Alternative antiandrogens to treat prostate cancer relapse after initial hormone therapy. J Urol 2004;171(2 Pt 1):679–683.
7. Hirano D, Minei S, Kishimoto Y, Yamaguchi K, Hachiya T, Yoshida T, Yoshikawa T, Endoh M, Yamanaka Y, Yamamoto T, Satoh Y, Ishida H, Okada K, Takimoto Y. Prospective study of estramustine phosphate for hormone refractory prostate cancer patients following androgen deprivation therapy. Urol Int 2005;75:43–49.
8. Nishimura K, Nonomura N, Satoh E, Harada Y, Nakayama M, Tokizane T, Fukui T, Ono Y, Inoue H, Shin M, Tsujimoto Y, Takayama H, Aozasa K, Okuyama A. Potential mechanism for the effects of dexamethasone on growth of androgen-independent prostate cancer. J Natl Cancer Inst 2001;93:1739–1746.
9. Hujanen ES, Terranova VP. Migration of tumor cells to organ-derived chemoattractants. Cancer Res 1985;45:3517–3521.
10. Cooper CR, Pienta KJ. Cell adhesion and chemotaxis in prostate cancer metastasis to bone: A minireview. Prostate Cancer Prostatic Dis 2000;3:6–12.
11. Baylink DJ, Finkelman RD, Mohan S. Growth factors to stimulate bone formation. J Bone Miner Res 1993;8(2 Suppl.):565–572.
12. Centrella M, Horowitz MC, Wozney JM, McCarthy TL. Transforming growth factor-beta gene family members and bone. Endocr Rev 1994;15:27–39.
13. Roberts AB, Wakefield M. The two faces of transforming growth factor β in carcinogenesis. Proc Natl Acad Sci USA 2003;100:8621–8623.
14. Yonou H, Horiguchi Y, Ohno Y, Namiki K, Yoshioka K, Ohori M, Hatano T, Tachibana M. Prostate-specific antigen stimulates osteoprotegerin production and inhibits receptor activator of nuclear factor-kappaB ligand expression by human osteoblasts. Prostate 2007;67:840–848.
15. Isaji M, Miyata H, Ajisawa Y. Tranilast: A new application in the cardiovascular field as an antiproliferative drug. Cardiovasc Drug Rev 1998;16:288–299.
16. Shime H, Kariya M, Orii A, Momma C, Kanamori T, Fukuhara K, Kusakari T, Tsuruta Y, Takakura K, Nikaido T, Fujii S. Tranilast inhibits the proliferation of uterine leiomyoma cells *in vitro* through G1 arrest associated with induction of $p21^{Waf1}$ and p53. J Clin Endocrinol Metab 2002;87:5610–5617.
17. Nie L, Oishi Y, Doi I, Shibata H, Kojima I. Inhibition of proliferation of MCF-7 breast cancer cells by a blocker of Ca^{2+}-permeable channel. Cell Calcium 1997;22:75–82.
18. Yashiro M, Chung YS, Sowa M. Tranilast (N-(3,4-dimethoxycinnamoyl) anthranilic acid) down-regulates the growth of scirrhous gastric cancer. Anticancer Res 1997;17:895–900.
19. Noguchi N, Kawashiri S, Tanaka A, Kato K, Nakaya H. Effects of fibroblast growth inhibitor on proliferation and metastasis of oral squamous cell carcinoma. Oral Oncol 2003;39:240–247.
20. Miwa S, Mizokami A, Keller ET, Taichman R, Zhang J, Namiki M. The bisphosphonate YM529 inhibits osteolytic and osteoblastic changes and CXCR-4-induced invasion in prostate cancer. Cancer Res 2005;65:8818–8825.
21. Lu Y, Zhang J, Dai J, Dehne LA, Mizokami A, Yao Z, Keller ET. Osteoblasts induce prostate cancer proliferation and PSA expression through inderleukin-6-mediated activation of the androgen receptor. Clin Exp Metastasis 2004;21:399–408.
22. Zhang J, Dai J, Qi Y, Lin DL, Smith P, Strayhorn C, Mizokami A, Fu Z, Westman J, Keller ET. Osteoprotegerin inhibits prostate cancer-induced osteoclastogenesis and prevents prostate tumor growth in the bone. J Clin Invest 2001;107:1235–1244.

23. Gerstenfeld LC. Osteopontin in skeletal tissue homeostasis. An emerging picture of the autocrine/paracrine functions of the extracellular matrix. J Bone Miner Res 1999;14:850–855.
24. Morgan DO. Principles of CDK regulation. Nature 1995;374: 131–134.
25. Peter M, Herskowitz I. Joining the complex: Cyclin-dependent kinase inhibitory proteins and the cell cycle. Cell 1994;79:181–184.
26. Platten M, Wild-Bode C, Wick W, Leitlein J, Dichgans J, Weller M. N-[3,4-dimethoxycinnamoyl]-anthranilic acid (tranilast) inhibits transforming growth factor-beta relesase and reduces migration and invasiveness of human malignant glioma cells. Int J Cancer 2001;93:53–61.
27. Rubin SJ, Hallahan DE, Ashman CR, Brachman DG, Beckett MA, Virudachalam S, Yandell DW, Weichselbaum RR. Two prostate carcinoma cell lines demonstrate abnormalities in tumor suppressor genes. J Surg Oncol 1991;46:31–36.
28. Ray S, Shyam S, Almasan A. S-phace checkpoints regulate Apo2 lagand/TRAIL and CPT-11-induced apoptosis of prostate cancer cells. Mol Cancer Ther 2007;6:1368–1378.
29. Cuptin JF, Cotter TG. Live and let die: Regulatory mechanisms in Fas-mediated apoptosis. Cell Signal 2003;15:983–992.
30. Blaszczyk N, Masri BA, Mawji NR, Ueda T, McAlinden G, Duncan CP, Bruchovsky N, Schweikert HU, Schnabel D, Jones EC, Sadar MD. Osteoblast-derived factors induce androgen-independent proliferation and expression of prostate-specific antigen in human prostate cancer cells. Clin Cancer Res 2004; 10:1860–1869.
31. Gleave M, Hsieh JT, Gao CA, von Eschenbach AC, Chung LW. Acceleration of human prostate cancer growth in vivo by factors produced by prostate and bone fibroblasts. Cancer Res 1991; 51:3753–3761.
32. Dallas SL, Zhao S, Cramer SD, Chen Z, Peehl DM, Bonewald LF. Preferential production of latent transforming growth factor beta-2 by primary prostatic epithelial cells and its activation by prostate-specific antigen. J Cell Physiol 2005;202:361–370.
33. Kassem M, Kveiborg M, Eriksen EF. Production and action of transforming growth factor-beta in human osteoblast cultures: Dependence on cell differentiation and modulation by calcitriol. Eur J Clin Invest 2000;30:429–437.
34. Liu W, Toyosawa S, Furuichi T, Kanatani N, Yoshida C, Liu Y, Himeno M, Narai S, Yamaguchi A, Komori T. Overexpression of Cbfa1 in osteoblasts inhibits osteoblast maturation and causes osteopenia with multiple fractures. J Cell Biol 2001;155:157–166.
35. Frank O, Heim M, Jakob M, Barbero A, Schäfer D, Bendik I, Dick W, Heberer M, Martin I. Real-time quantitative RT-PCR analysis of human bone marrow stromal cells during osteogenic differentiation *in vitro*. J Cell Biochem 2002;85:737–746.
36. Yashiro M, Murahashi K, Matsuoka T, Nakazawa K, Tanaka H, Osaka H, Koyama T, Ohira M, Chung KH. Tranilast (N-3,4-dimethoxycinamoyl anthranilic acid): A novel inhibitor of invasion-stimulating interaction between gastric cancer cells and orthotopic fibroblasts. Anticancer Res 2003;23:3899–3904.
37. el-Shirbiny AM. Prostatic specific antigen. Adv Clin Chem 1994; 31:99–133.
38. Kusama H, Kikuchi S, Tazawa S, Katsuno K, Baba Y, Zhai YL, Nikaido T, Fujii S. Tranilast inhibits the proliferation of human coronary smooth muscle cell through the activation of p21waf1. Atherosclerosis 1999;143:307–313.
39. Cheng I, Stram DO, Penny KL, Pike M, Le Marchand L, Kolonel LN, Hirschhorn J, Altshuler D, Henderson BE, Freedman ML. Common genetic variation in IGF1 and prostate cancer risk in the multiethnic cohort. J Natl Cancer Inst 2006;18:123–134.
40. Fan J, Stanfield J, Guo Y, Karam JA, Frenkel E, Sun X, Hsieh JT. Effect of trans-2,3-dimethoxycinnamoyl azide on enhancing antitumor activity of romidepsin on human bladder cancer. Clin Cancer Res 2008;15:1200–1207.